Supporting Information:

Equipments

The melting point of the generated imine ligand and the decomposition temperatures of its complexes were ascertained using a melting point instrument (Gallenkamp, UK). The KBr pellets' infrared spectra were recorded using a Shimadzu FTIR-8300 spectrophotometer. ^{1}H and ^{13}C NMR spectra were obtained in deuterated dimethylsulfoxide (DMSO) solutions using a Bruker Avance DPX-500 spectrometer. All of the scanning UV-visible spectra in DMF were recorded using 10 mm matched quartz cells and a PG spectrophotometer type T + 80. At Cairo University's main laboratory, elemental studies were conducted using a PerkinElmer 240c elemental analyzer. Magnetic susceptibility was measured using a Gouy balance, and diamagnetic corrections were made using Pascal's constants. The molar conductivity was measured using a JENWAY 4510 conductivity meter. The absorbance values of 5×10^{-3} M for each complex were determined at different pH ranges. The pH levels were determined using a number of Britton universal buffers. An ADWA AD1000 and AD1020 pH meter was used to measure pH at 298 K using a CL-51B combination electrode that had been calibrated against standard buffers (pH 4.02 and 9.18) beforehand.

c13_su DMSO {D:\NMR Data} Student 2

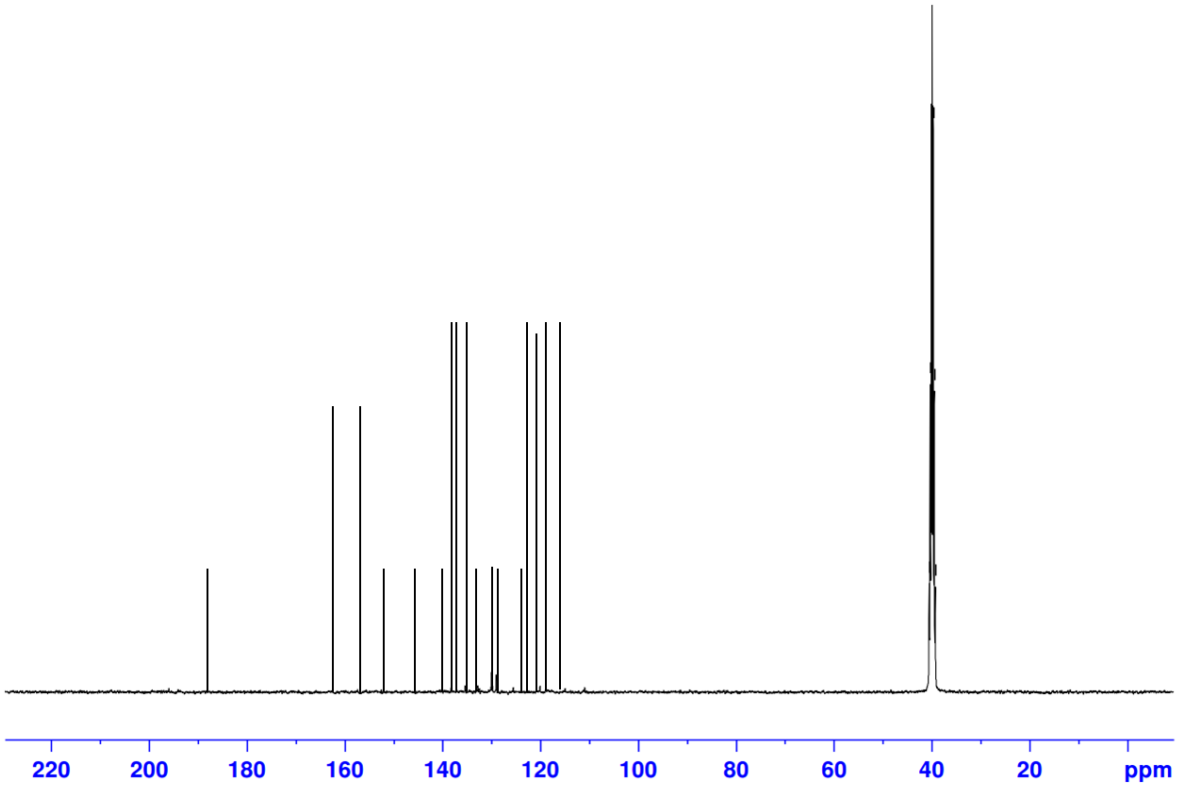


Figure S1: ^{13}C NMR spectra of the L imine pro-ligand

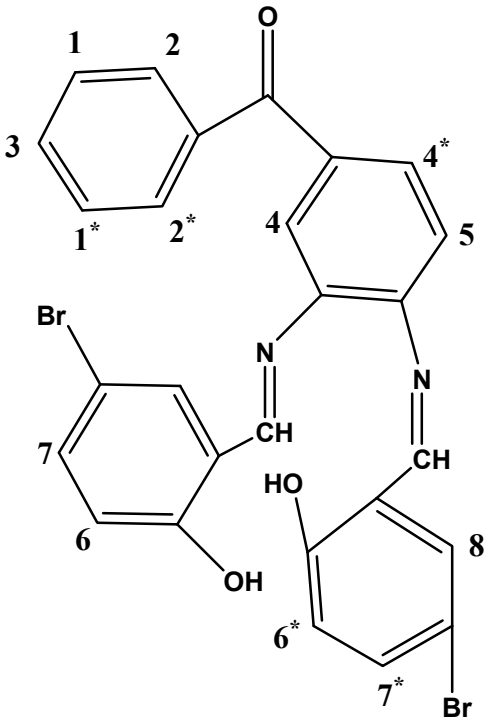
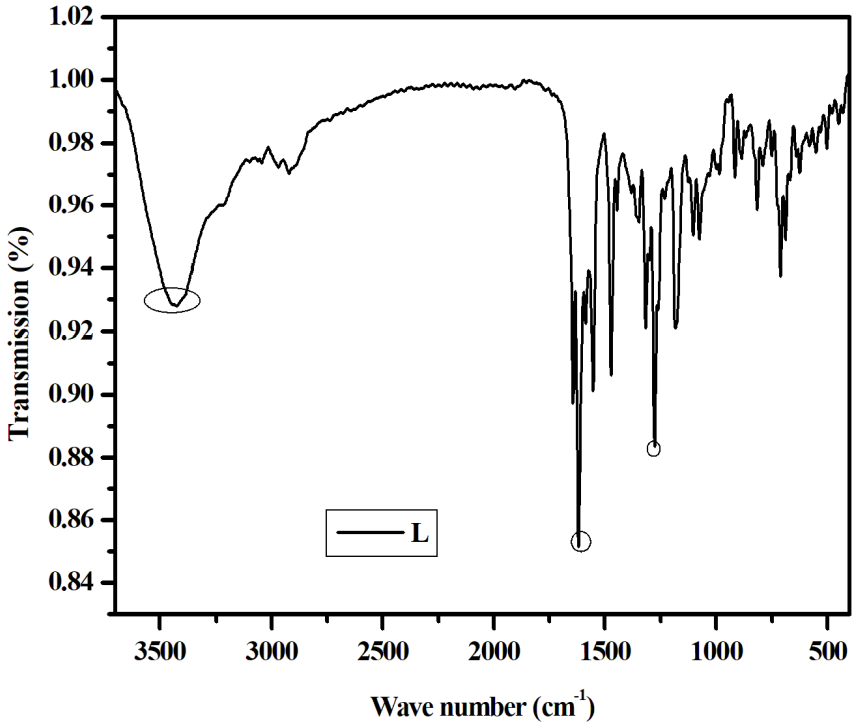


Figure S2: proposal structure of L imine ligand



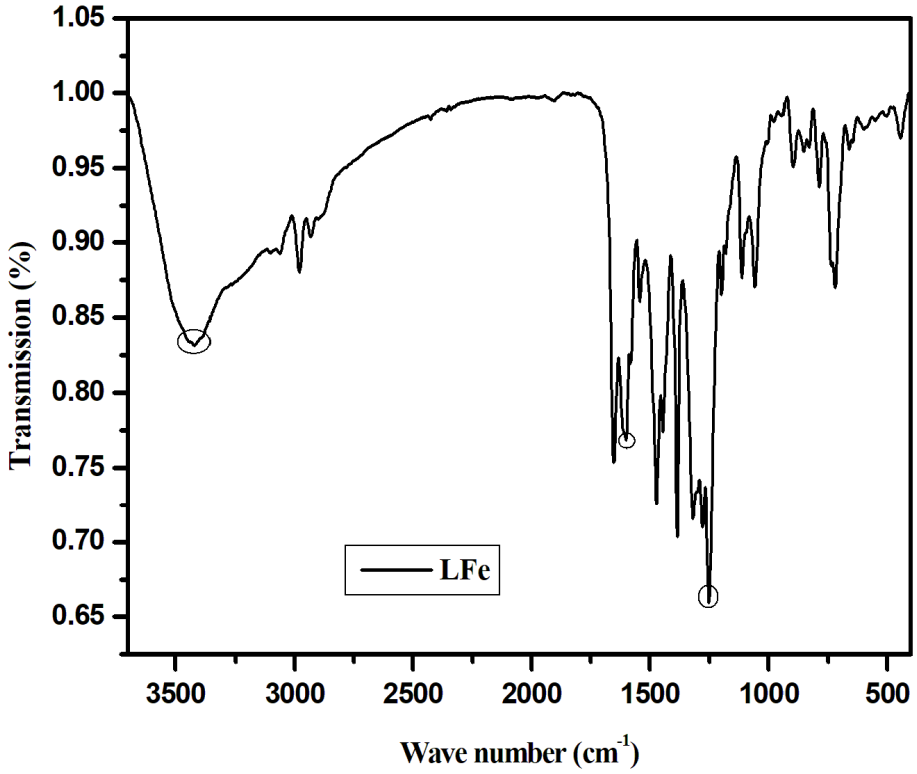
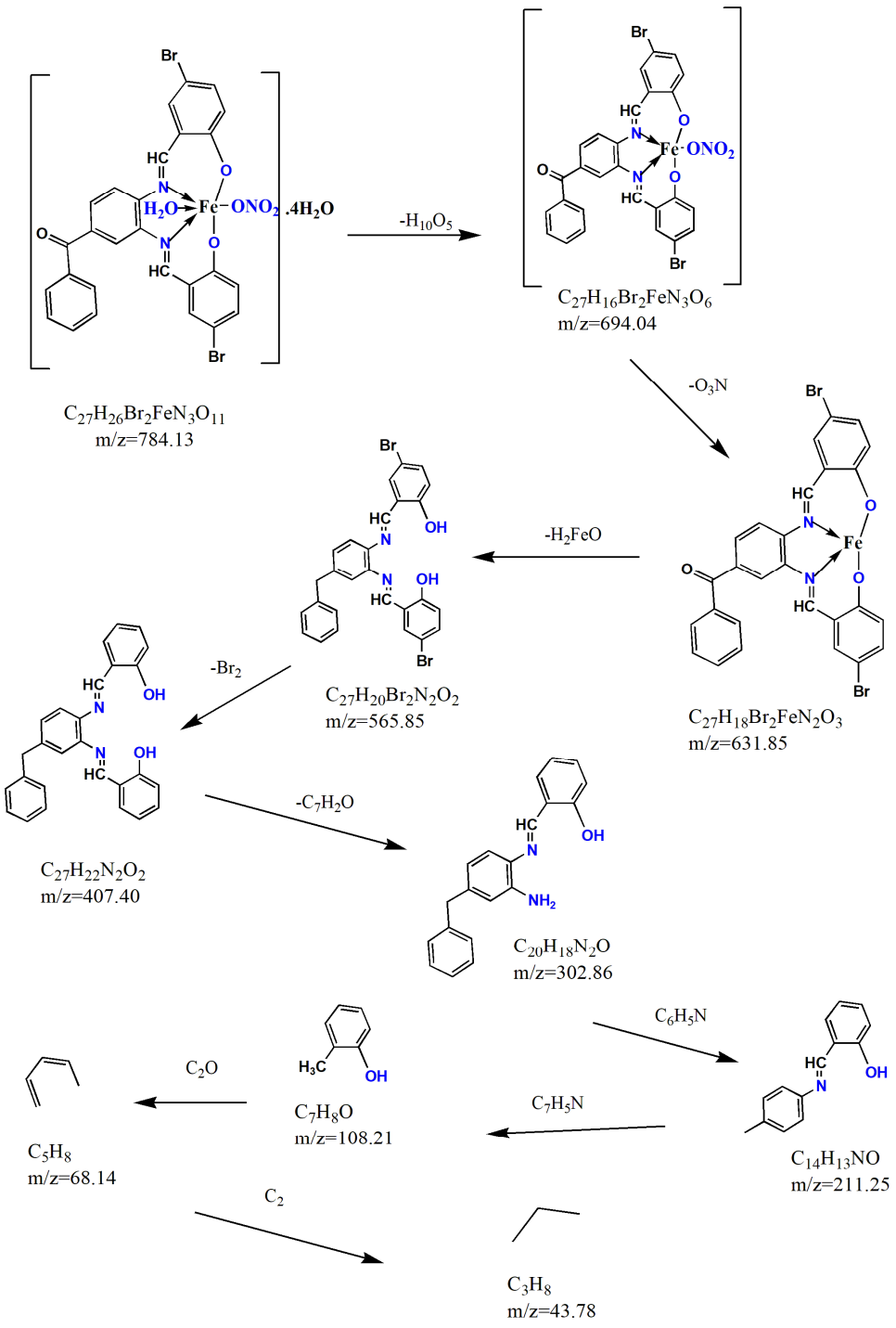


Figure S3: FT-IR spectrum of L imine ligand and its complex



SCHEME S1: Fragmentation pathway of LFe complex. Below each structure, the precise masses of the particles and their chemical formulas are displayed.

2. 6. Materials and Procedure in corrosion and charge discharge studies

Pure nickel metal sample with a surface area of one centimeter serves as the working electrode. Several dosages of the ligand and its complex were used to assess the inhibitory effect of the L ligand and FeL complex on rate of nickel corroding in acidic media. (1×10^{-5}, 5×10^{-5}, 1×10^{-4}, 5×10^{-4}, 1×10^{-3} M) were consumed. Corroding-causing fluid contained 0.5 M sulfuric acid (BDH 99.9%). Using Tafel plot on Ni metal, electrochemical behaviors of the ligand and its complex in the acidic media were discovered. Additionally, [electrochemical impedance spectroscopy] was utilized to highlight how well additives inhibited nickel corroding reaction. A VersaSTAT 4 potentiostat/Galvanostat was employed for the electrochemical investigations. A Pyrex glass cell with three electrodes has been employed. [The cell] layout was created using data that has previously been released. Tafel curves' cathodic as well anodic reaction branches are obtained utilizing scanning speed of 10 mV/s as well potential around ±0.25 V, respectively, with regard to corroding equilibrium potential (E_{corr}). Experiments have been carried out to investigate [polarization resistance of Ni in the acidic medium in the absence and presence of different dosages of the additives at open circuit potential of corroding (E_{corr}), utilizing [impedance spectroscopy] (EIS) at frequencies between 10 kHz and 5 mHz with an amplitude of 10 mV. After corroding tests, the JEOL-5300 (SEM) is appropriately used to detect and determine the surface morphology of each sample. An Electrochemical cell made of nickel specimens was used. with size of centimetre, a platinum auxiliary electrode (CE), and Ag/AgCl as the reference electrode (RE).

Finding and discussion

Table S1: Tafel parameters for Nickel metal in 0.5 M H_2SO_4 without additives at distinct temperatures.

Temp.	E_{corr} (V)	I_{corr} ($\mu A\ cm^{-2}$)	β_a (V/decade)	β_c (V/decade)	Θ	η %
Blank						
25 ºC	-0.228	616.6	19.5	-4.38	-	-
35 ºC	-0.228	1202.3	14.6	-4.12	-	-
45 ºC	-0.217	3548	6.8	-4.8	-	-
55 ºC	-0.214	7400	10.5	-4.2	-	-

Table S2: Activation energy data (E_a) of Ni in [0.5 M H_2SO_4] solution, while additives are absent and present in multiple doses.

$C_{inh.}$ mol/l	E_a kJmol^{-1} (L)	E_a kJmol^{-1} (FeL)
Blank	30.3	30.3
1×10^{-5}	37.1	39.2
1×10^{-4}	42.9	48.3
1×10^{-3}	45.8	50.7

Table S3: EDAX analysis for the oxide layers formed on Ni surface in 0.5 M H_2SO_4.			
In the absence of the inhibitor			
Element	Line	Mass%	Atom%
O	K	35.64 ± 0.13	48.65 ± 0.29
S	K	6.60 ± 0.07	7.40 ± 0.08
Ni	K	57.76 ± 0.37	43.95 ± 0.23
Total		100.00	100.00

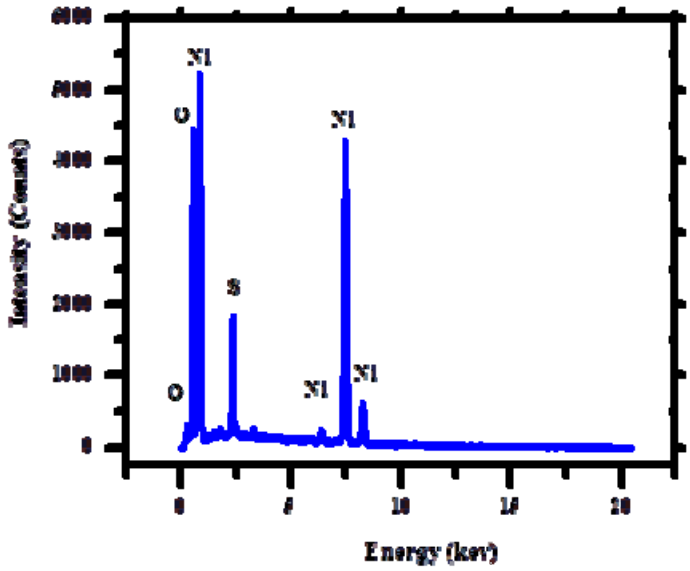


Figure S4: EDAX analysis for oxide layers formed on Ni exterior side in 0.5 M H_2SO_4.

3.2.5. Charge discharge studies:

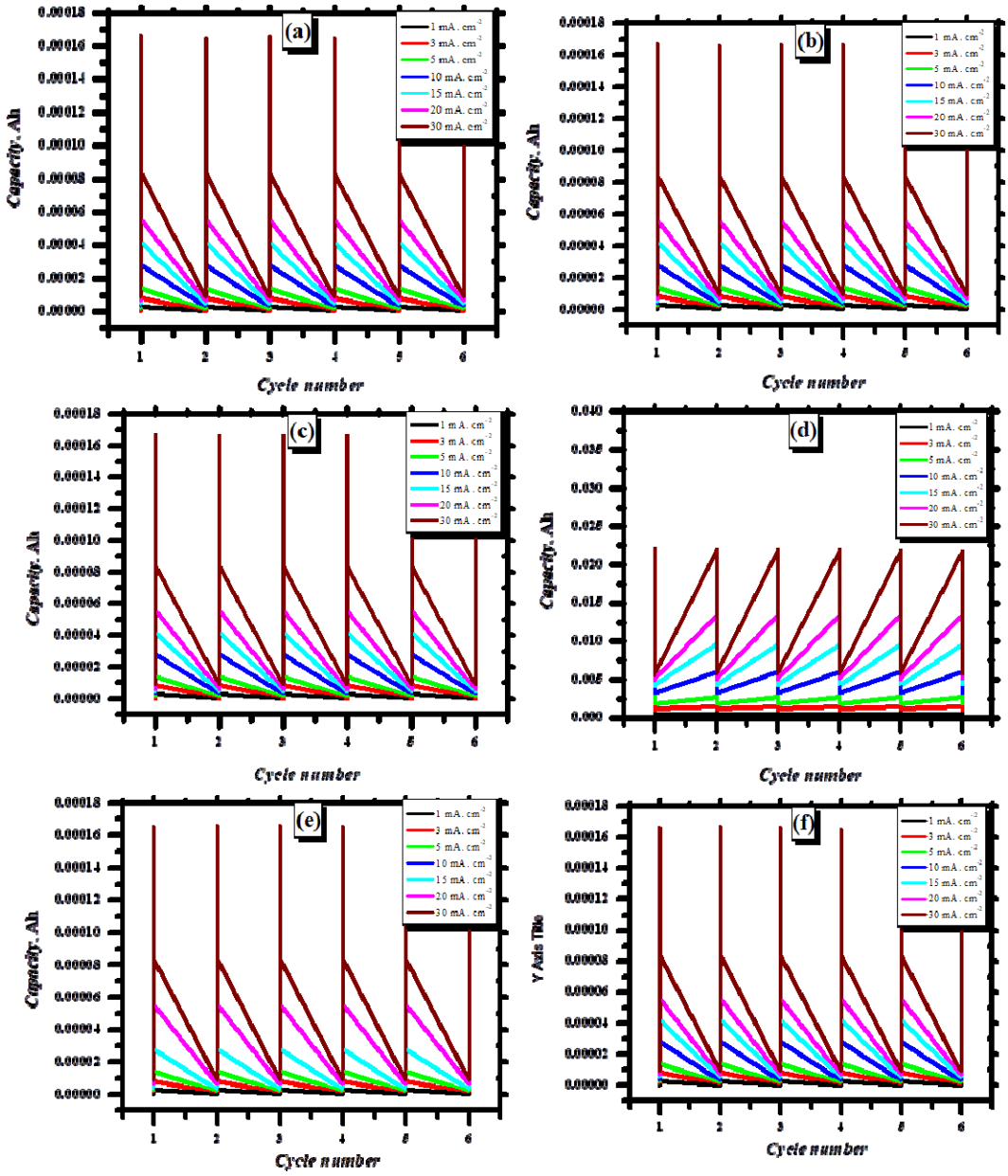


Figure S5: Change of capacity during six cycles for Ni metal in 0.5 M H_2SO_4 (a) without and with 1×10^{-5} M (b) 5×10^{-5} M (c), 1×10^{-4} M (d), 5×10^{-4} M (e), and 1×10^{-3} M (f) of L at applied various current densities.

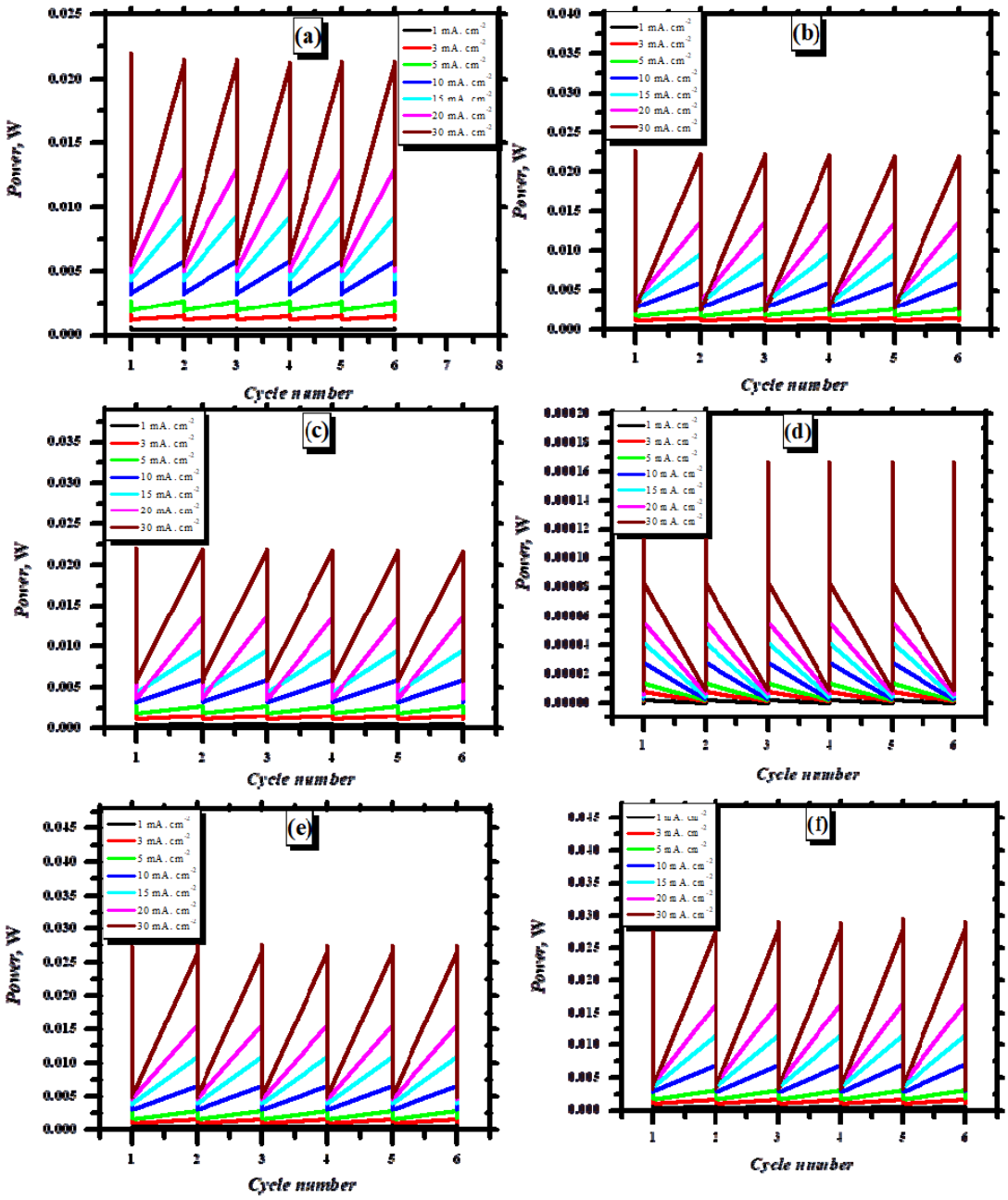


Figure S6: Power variation of Ni metal during six cycles in 0.5 M H_2SO_4 (a) without and with 1×10^{-5} M (b) 5×10^{-5} M (c), 1×10^{-4} M (d), 5×10^{-4} M (e), and 1×10^{-3} M (f) of L at applied various current densities.

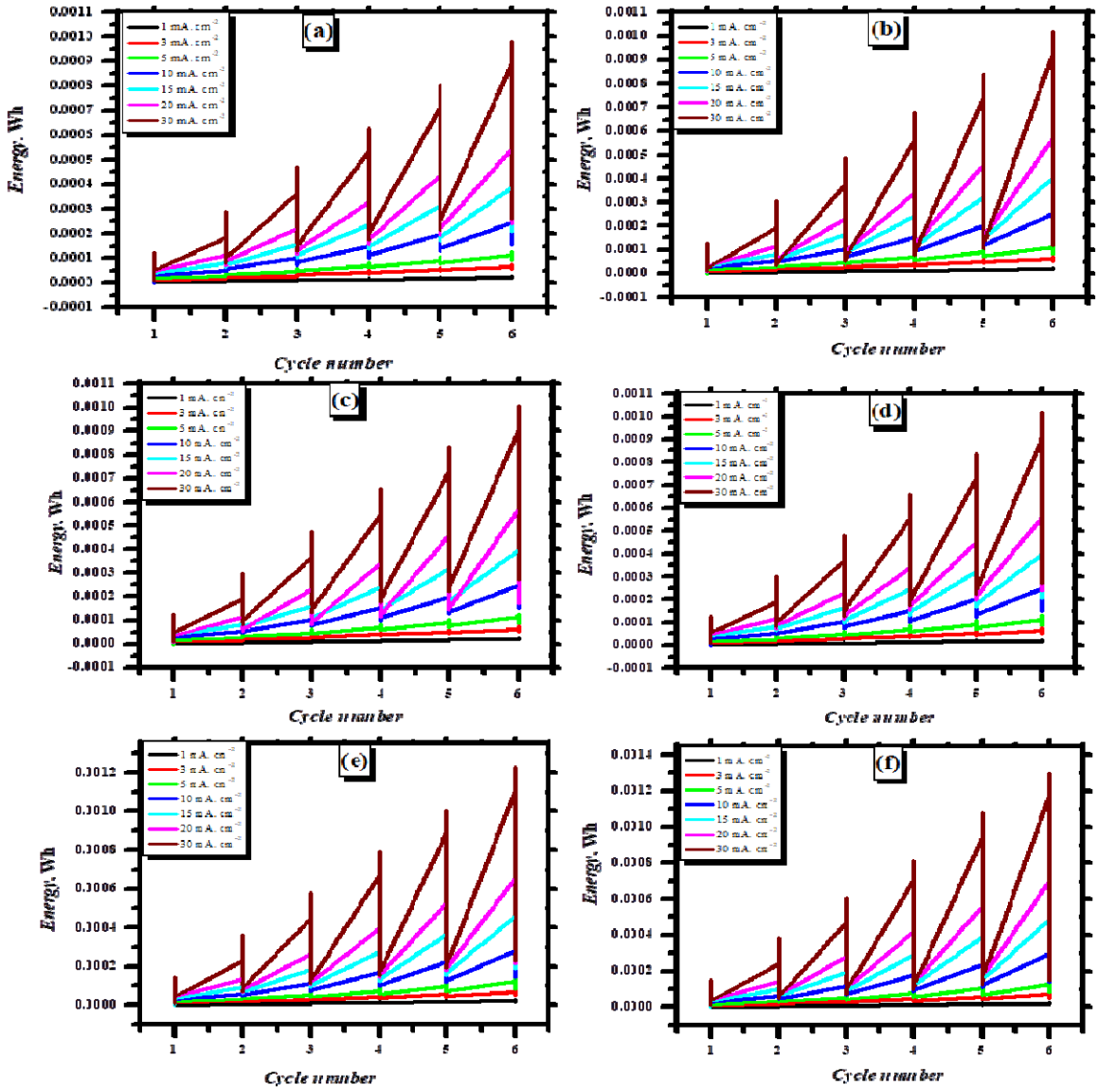


Figure S7: Change of Energy with cycle number for Ni metal in 0.5 M H_2SO_4 (a) without and with 1×10^{-5} M (b) 5×10^{-5} M (c), 1×10^{-4} M (d), 5×10^{-4} M (e), and 1×10^{-3} M (f) of L at applied various current densities.

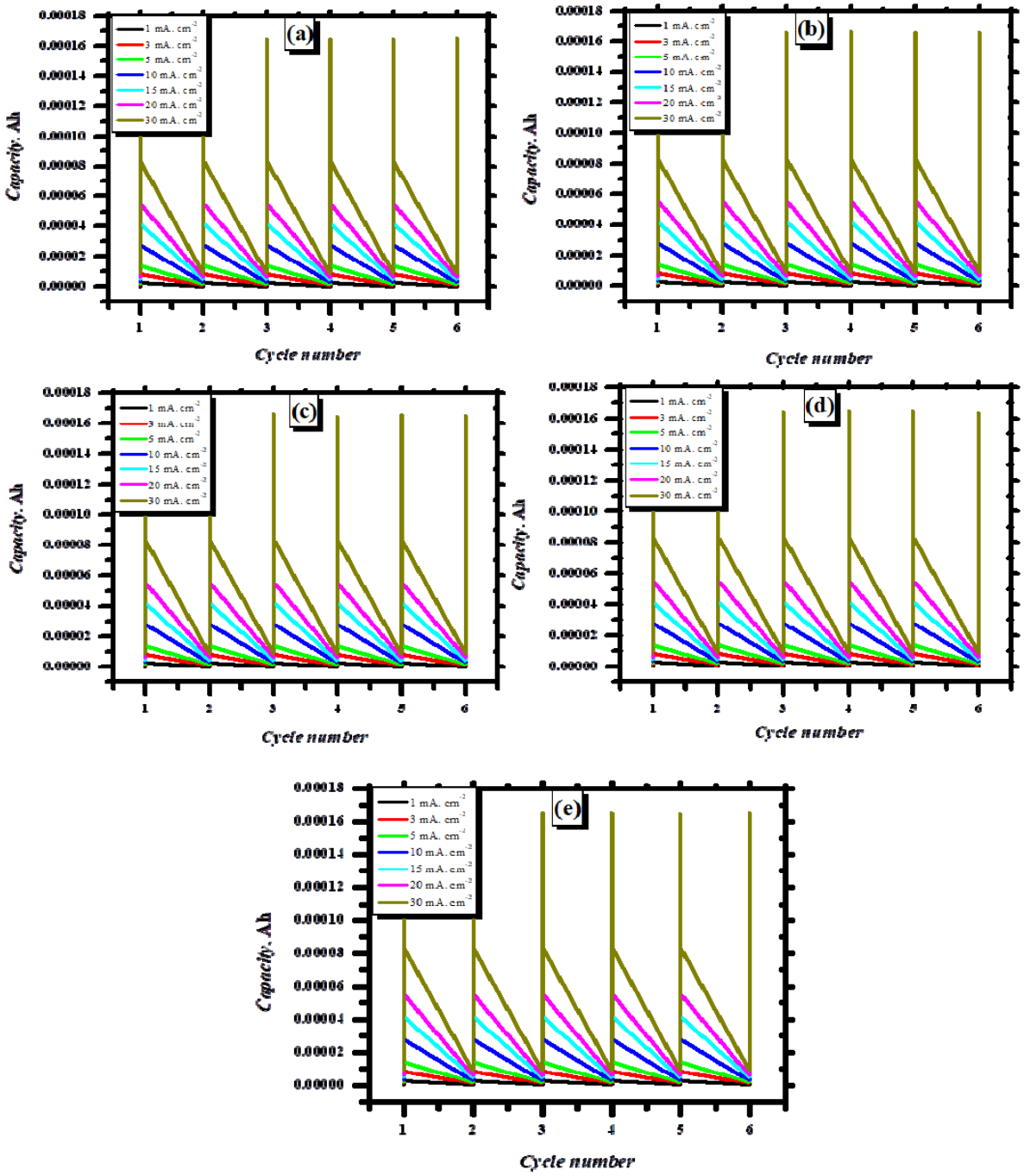


Figure S8: Change of Capacity during six cycles for Ni metal in 0.5 M H_2SO_4 with 1×10^{-5} M (a) 5×10^{-5} M (b), 1×10^{-4} M (c), 5×10^{-4} M (d), and 1×10^{-3} M (e) of FeL at applied various current densities.

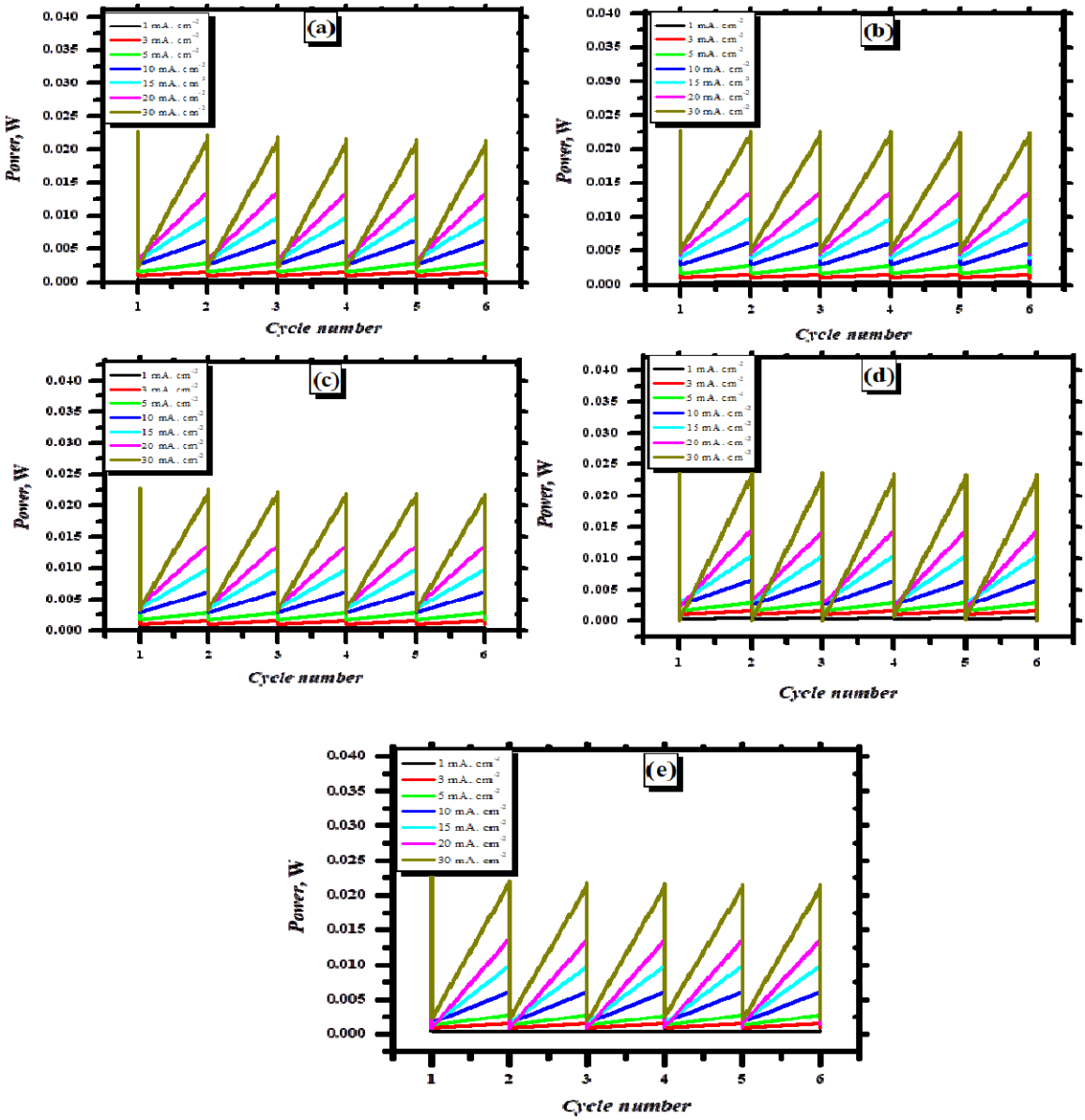


Figure S9: Power variation during six cycles for Ni metal in 0.5 M H_2SO_4 with 1×10^{-5} M (a) 5×10^{-5} M (b), 1×10^{-4} M (c), 5×10^{-4} M (d), and 1×10^{-3} M (e) of FeL at applied various current densities.

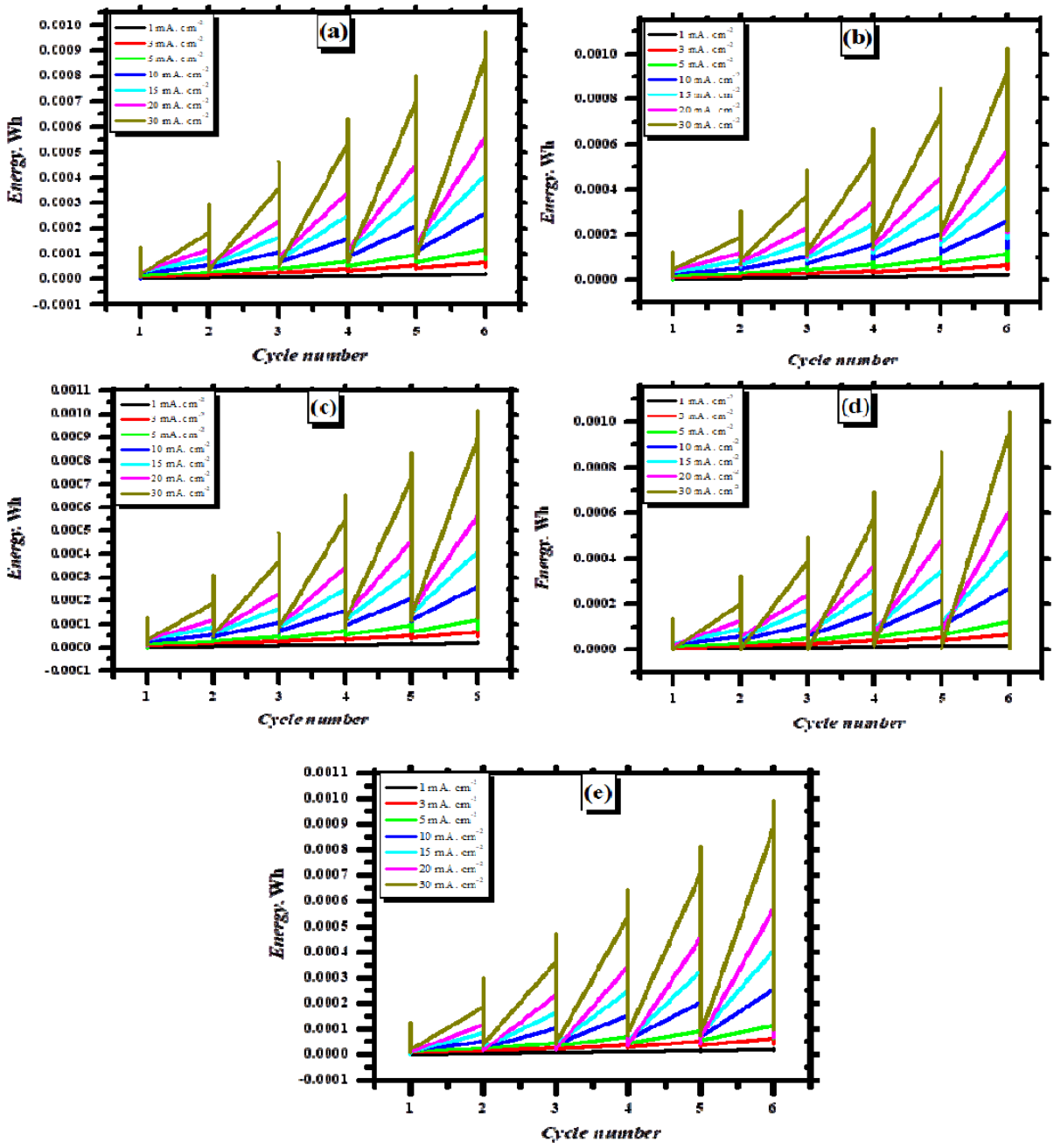


Figure S10: Change of Energy with time for Ni metal in 0.5 M H_2SO_4 with 1×10^{-5} M (a) 5×10^{-5} M (b), 1×10^{-4} M (c), 5×10^{-4} M (d), and 1×10^{-3} M (e) of FeL at applied various current densities.